Wind tunnel experiments on visible plume from a cooling tower

Takenobu Michioka, Ayumu Sato, Takao Kanzaki and Kouichi Sada

Environmental Science Research Laboratory, Central Research Institute of Electric Power Industry (CRIEPI), Chiba, Japan; E-mail: michioka@criepi.denken.or.jp

ABSTRACT

We developed a new method for a wind tunnel experiment to predict a visible plume region from a mechanical-draft cooling tower. The diffusions of water vapor and heat emitted from the cooling tower in the wind tunnel are tracked using a tracer gas. The instantaneous concentration of the tracer gas is measured using high-response flame ionization detectors. A moist plume-induced fog is generated whenever the instantaneous water vapor mixing ratio estimated using the tracer gas at measurement points is larger than the saturation water vapor mixing ratio. Furthermore, since the instantaneous fog is retained for a finite period, it is assumed that the instantaneous fogging region is included in the visible plume region. To estimate the accuracy of the present method, the visible plume region in the wind tunnel experiment is compared with the observations of the mechanical-draft cooling tower at the Benning Road plant. The results show that the visible plume length and height are in good agreement with the observations, and that the present wind tunnel method can well describe the visible plume region from the cooling tower.

1. Introduction

Visible plumes from a wet cooling tower produce some significant atmospheric effects, such as the reduction of visibility to air and ground, ice formation on surfaces, cloud initiation, and augmentation of precipitation. It is therefore of great importance to predict the visible plume region from the cooling tower in environmental impact assessment.

A wind tunnel experiment is considered to be one of the predominant methods. Kennedy and Fordyce[1] conducted wind tunnel experiments for a mechanical cooling tower and determined downwind temperature distributions and interference characteristics of buoyant jets. Andreopoulos[2),3] performed the wind tunnel experiment and discussed the behavior of the heat emitted from the cooling tower. Many researchers have investigated the scalar (temperature) behavior from the cooling tower, but no one has estimated the visible plume region generated from the vapor of the cooling tower.

The purpose of the present study is to develop a new method for a wind tunnel experiment to predict the visible plume region from a mechanical-draft cooling tower. The diffusions of water vapor and heat emitted from the cooling tower in the wind tunnel were tracked using a tracer gas. The instantaneous concentration of the tracer gas was measured using high-response flame ionization detectors. The results obtained by the present wind tunnel

experiments were compared with the observations.

2. Wind tunnel experiment

Experiments were conducted in the wind tunnel facility at Komae Research Laboratory of Central Research Institute of Electric Power Industry (CRIEPI). This wind tunnel has a 3m-wide, 1.5m-high and 20m-long test section. A free stream velocity of U_0= 1.0m/s was employed and roughness elements with L-shaped cross sections were set on the wind tunnel floor at the entrance of the test section. The position of tracer gas release was 4.7 m downstream of the entrance of the wind tunnel test section, and at the horizontal center of the wind tunnel test section y = 0 m. One model stack corresponding to some stacks of the cooling tower was located at x = 0 m. A mixture of air, helium (He) and ethylene (C_2H_4) was released from the model stack as the tracer gas, from the height of z = 0.02 m, which corresponds to the stack height of the mechanical cooling tower. The instantaneous velocity was measured using a laser Doppler velocimeter (LDV). The instantaneous concentration of the tracer gas was measured using a high-frequency-response flame ionization detector at several vertical cross sections downwind of the stack. The schematic of the concentration measuring system is shown in Figure 1. The sample gas emitted from the stack was aspirated at a very high speed through a short, narrow metallic tube into the sampling chamber connected to the carriage system, which can be moved to arbitrary positions in the test section. The aspirated tracer gas was mixed with the fuel gas and burned in the chamber. The calibration of the detector was carried out using a test gas of known composition before each experiment and the detector was found to have linear calibration curves up to about 2,000 ppm. The concentration data of the tracer gas were obtained at each measuring point.

3. Similarity criteria with atmosphere

To simulate the vapor emitted from the cooling tower in wind tunnel experiment, some similarity criteria in the wind tunnel must coincide with that in atmosphere. The following similarity criteria are considered. The first criterion is based on the bulk Richardson number:

$$R_{ib} = \frac{\beta g \Delta T D}{V^2}, \tag{1}$$

which represents the ratio of the buoyancy effect caused by the temperature (density) difference to the flow inertial force. Here, β is the thermal volumetric expansion coefficient, g is gravitational acceleration, ΔT is the temperature difference between atmosphere and the exit of the stack, D is the stack diameter, and V is the velocity of emission from the stack. When the same values of the bulk Richardson number are attained for the wind tunnel and atmosphere,

$$\frac{\Delta T_m}{\Delta T_p} = \left(\frac{V_m}{V_p} \right)^2 \frac{D_p}{D_m} \tag{2}$$

can be obtained. The subscripts p and m indicate atmosphere and the wind tunnel, respectively.

The temperature difference, ΔT, is related to the density difference, $\Delta\rho$, as

$$\Delta T = -T_p \frac{\Delta\rho}{\rho_m}. \tag{3}$$

Hence, the density of gas emitted from the stack in the wind tunnel experiment is determined using

$$\rho_{cm} = \frac{\rho_p}{1 + \frac{\Delta\rho_p}{\rho_{cp}} \left(\frac{V_m}{V_p} \right)^2 \frac{D_p}{D_m}}. \tag{4}$$

The second criterion is based on the Reynolds number,

$$R_e = \frac{DV}{\gamma}, \tag{5}$$

where ν is the kinematic viscosity. The second condition cannot be satisfied between atmosphere and the wind tunnel. However, this criterion is satisfied under the condition that *Re* is larger than 300.

Considering the two similarity criteria and the performance of the wind tunnel facility, wind tunnel experiments were conducted under the conditions of $U=V=$ 1.0m/s, $\Delta\rho = 0.5359$, $D = 29.8\times10^{-3}$, D_p/D_m = 1/1000 and $R_e \approx 20000$. The details of the conditions are listed in Table 1.

4. Determination of a visible plume region

Since the vapor mixing ratio is tracked using tracer gas in the present experiment, the visible plume region cannot be directly estimated. In the present experiment, the visible plume region was predicted as follow.

The vapor mixing ratio at the measuring point, *M,* is tracked using the concentration of a tracer gas, *C*. The ratio of *C* to the initial concentration, C_c , is

$$R_d = \frac{C}{C_c}. \tag{6}$$

The vapor mixing ratio at the measuring point is estimated using

$$M = R_d (M_c - M_a) + M_a, \tag{7}$$

where M_a and M_c are the vapor mixing ratios in atmosphere and at the exit of the cooling tower, respectively.

It is provided that the visible plume appears under the condition of $M \geq M_S$ where M_s is the saturated mixing ratio. To estimate M_s at the measuring point, the temperature and pressure are needed. In the case of the temperature, the heat diffusivity is almost equal to the material diffusivity, so that temperature was also tracked using the same tracer gas. However,

since the temperature usually has a vertical distribution in the atmospheric boundary layer, the potential temperature was applied in this method instead of the temperature. The potential temperature can be defined as

$$\theta = T\left(\frac{P_{00}}{P}\right)^{k}, \qquad k = \frac{R}{C_p}, \tag{8}$$

where P_{00} is the reference pressure, P is the pressure at the measuring point, R is the gas constant and C_p is the specific heat at a constant pressure. The potential temperature at the measuring point is estimated using

$$\theta = R_d(\theta_c - \theta_a) + \theta_a, \tag{9}$$

where θ_c and θ_a are the potential temperatures in atmosphere and at the exit of the cooling tower, respectively. The pressure at the measuring point is given as

$$P = P_g(1.0 - 0.0065\frac{z}{T_g})^{5.267}, \tag{10}$$

where z is the height, and P_g and T_g are pressure and temperature at the ground level, respectively. The saturated vapor pressure relevant to temperature, T, is obtained using Sontang's equation,

$$\begin{aligned} P_s = \exp(&-6096.9385T^{-1} + 21.2409642 - 2.71193\times10^{-2}T \\ &+1.673952\times10^{-5}T^2 + 2.433505\times\ln(T)). \end{aligned} \tag{11}$$

Using the above relation, the saturated mixing ratio, M_s, can be obtained as

$$M_s = 0.622\frac{P_s}{P - P_s}. \tag{12}$$

As explained above, the visible plume was generated under the condition that the vapor mixing ratio, M, at the measuring point is larger than the saturated mixing ratio, M_s.

5. Results and discussion

The basic behavior of the flow and the scalar are discussed before predicting the visible plume region in the wind tunnel. Figure 2 shows the vertical distributions of mean wind velocity and the rms values of turbulent intensities at x/H_c = 5, 25. These velocities and turbulent intensities are normalized by the free stream velocity, U_0, and vertical distance is normalized by the stack height, H_c. The black circles display the no-stack (flat plane) data. Since the jet from the stack is injected perpendicularly to the wind direction, the wind velocity becomes smaller in the region of $z/H_c < 10.0$ compared with that in the no-stack (flat) case. On the other hand, the turbulent intensities become larger owing to the steep vertical slope of the mean velocity. These trends are in good agreement with the experimental results obtained by Andreopoulos[2),3)].

Figure 3 shows the vertical distributions of mean concentration at x/H_c = 5, 15, 25. The mean concentration is normalized by the concentration at the exit of the stack, C_c. The vertical shapes of the mean concentration are almost equal to a Gaussian distribution and the vertical position of the maximum values become large with downwind distance. The upward curve of the maximum values coincides with Briggs 2/3 law[4] (the figure is not shown here). This indicates that the normal upward trajectory of the tracer gas could be simulated in the present wind tunnel.

The visible plume region was estimated by the method explained in Section 4. The visible plume length, L_v, and height, H_v were defined as the lengths from the center of the cooling tower to the downwind edge of the visible plume and from the ground to the center of the visible plume, respectively (shown in Figure 4). Figure 5 shows the visible plume length and height in the range of relative humidity from 0.5 to 0.8 at ground level and the black circles mark the observations (PEPCO BENNING ROAD POWER STATION[5),6)]). The atmospheric and emitted conditions in the observations are listed in Table 2. Although our experimental conditions in the present wind tunnel do not completely coincide with these observations, some observed data, which nearly equivalent to total volume flux emitted from the stack and the bulk Richardson number in our experiment, were selected.

First, the visible plume region is defined as the region where the mean vapor mixing ratio is larger than the saturated mixing ratio. These results (black square in Figure 5) give good agreement with the visible plume height, but considerably underestimate the visible plume length. These results indicate that the visible plume region cannot be estimated from only the mean vapor mixing ratio. Next, the instantaneous fogging region is included in the visible plume region because the instantaneous fog does not evaporate instantaneously but is retained for a finite period. This means that whenever the instantaneous mixing ratio is larger than the saturated mixing ration, the visible plume is generated. Under this assumption, the results (black circle in Figure 5) are in good agreement with the observations for both visible height and length, and the present method, using instantaneous vapor mixing ratio, can accurately predict the visible plume region.

In Figure 5, the visible plume length and height in the range of high relative humidity of $R_H > 0.8$ could not be displayed. Because, it is assumed in the present method that the cloud is generated at high position of a few meters under the condition of high relative humidity at the ground level, on the basis of the assumption of a constant vapor mixing ratio in atmosphere, and whether the visible plume is generated by the vapor from the cooling tower or not cannot be confirmed. However, even in the field observation, accurate visible plume length and height cannot easily be estimated since the visible plume usually reaches at the cloud ceiling under the condition of high relative humidity. This indicates that the visible plume region at such a high position need not be predicted. In addition, since the visible plume region at a lower position can actually be predicted using the present method, it is possible to estimate the reduction of visibility on elevated roads in environmental impact assessment.

6. Conclusions

We developed a new method for a wind tunnel experiment to predict the visible plume region from a mechanical-draft cooling tower. The diffusions of water vapor and heat emitted from the cooling tower in the wind tunnel were tracked using a tracer gas. A moist plume-induced fog was generated whenever the instantaneous water vapor mixing ratio, estimated using the tracer gas at measurement points, is larger than the saturation water vapor mixing ratio. Furthermore, since the instantaneous fog is retained for a finite period, it was assumed that the instantaneous fogging region is included in the visible plume region. The visible plume length and height estimated using the present wind tunnel method were in good agreement with the observations. Hence, the present wind tunnel method can accurately predict the visible plume region from the cooling tower and it is a promising method in environmental impact assessment.

Reference

1) Kennedy, J. F. and Fordyce, H., 'Plume recirculation and interference in mechanical-drift cooling towers,' in Cooling tower environment (1974) 58-87.
2) Andreopoulos, J., 'Wind tunnel experiments on cooling tower plumes: Part 1-Uniform Crossflow,' ASME Journal of heat transfer, 111 (1989) 941-948.
3) Andreopoulos, J., 'Wind tunnel experiments on cooling tower plumes: Part 2-in a nonuniform crossflow of boundary layer type,' ASME Journal of heat transfer, 111 (1989) 949-955.
4) Briggs, G. A., Plume Rise, U. S. Atomic Energy Commission, Division of Technical Information (1969).
5) Meyer, J. H., Eagles, T. W., Kohlenstein, L. C., Kagan, J. A. and Stanboro, W. D., 'Mechanical-draft cooling tower visible plume behavior: measurements, models, predictions,' in Cooling tower environment (1974) 307-352.
6) Policastro, A. J., Carhart, R. A. and Wastag, M. 'Studies on mathematical models for characterizing plume and drift behavior from cooling towers: Volume 4', EPRI CS-1683, (1981).

Tabele 1 Specification of cooling tower and wind condition in wind tunnel experiments.

Parameters	Values
Free wind velocity U_o (m/s)	1.0
Stack diameter D (m)	29.8×10^{-3}
Stack heghit H_c (m)	2.0×10^{-2}
Emitted velocity V_c (m/s)	1.0
Emitted density ρ_c (kg/m^3)	0.6687
Density difference $\Delta\rho$ (kg/m^3)	0.5359
Representive temparature T_a (K)	297.15
Bulk Richardson number R_{ib}	0.228

Table 2 Observation of exit gas and meteorological conditions.

Site	Height of Tower (m)	DATE	Weather condition		Exit Gas condition		Ri_b
			Wind speed (m/s)	Relative Humidity (%)	Ambient Temperature (^oC)	Exit Volume flux (m^3/s)	
Washington [5),6)] (USA)	18.29	1973/10/31	3.1	58	16.5	4431	0.232
		1973/11/2	3.1	52	15.3	4410	0.218
		1973/11/13	3.1	46	14.5	5215	0.218
		1973/11/14	5.1	63	18	4888	0.142

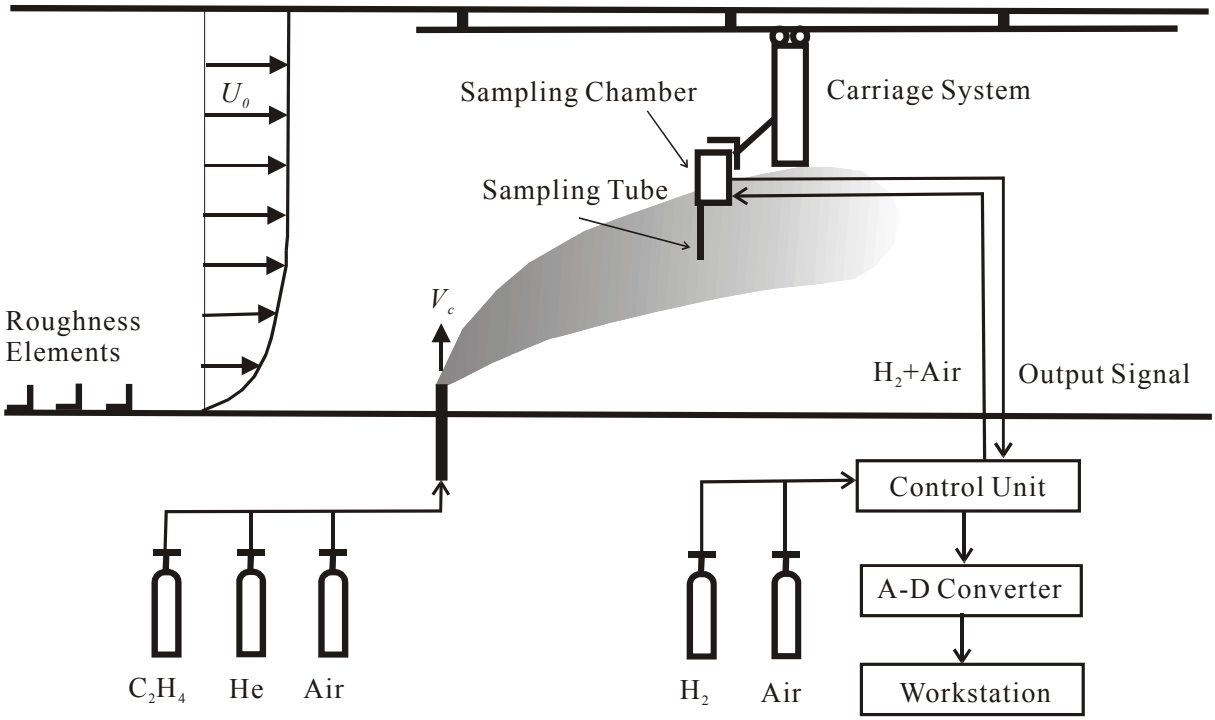

Figure 1 Schematic of the concentration measuring system in wind tunnel experiment.

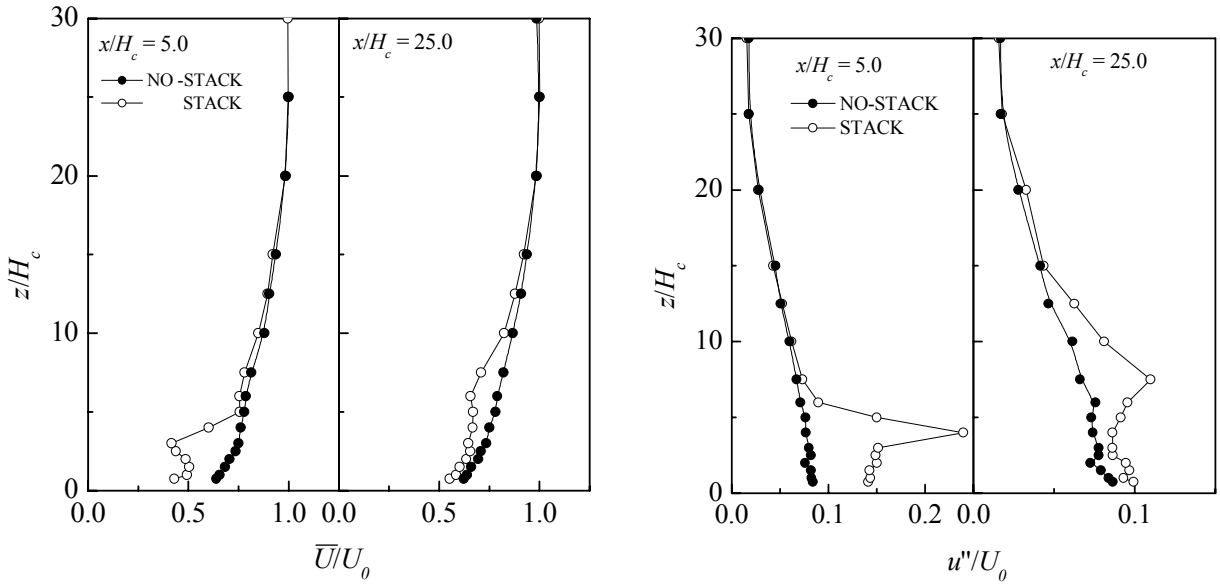

(a) mean wind velocity (b) rms value of turbulent intensity

Figure 2 Vertical distributions of the mean wind velocity and the rms value of turbulent intensity.

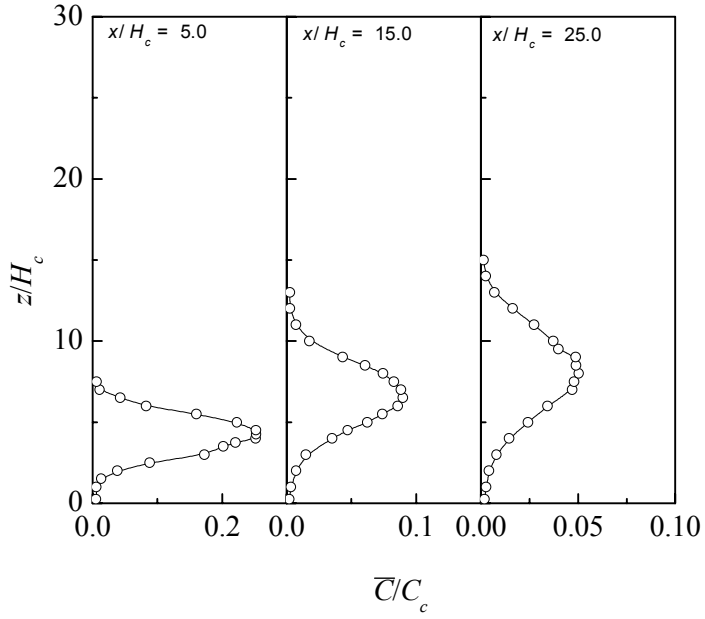

Figure 3 Vertical distributions of the mean concentration.

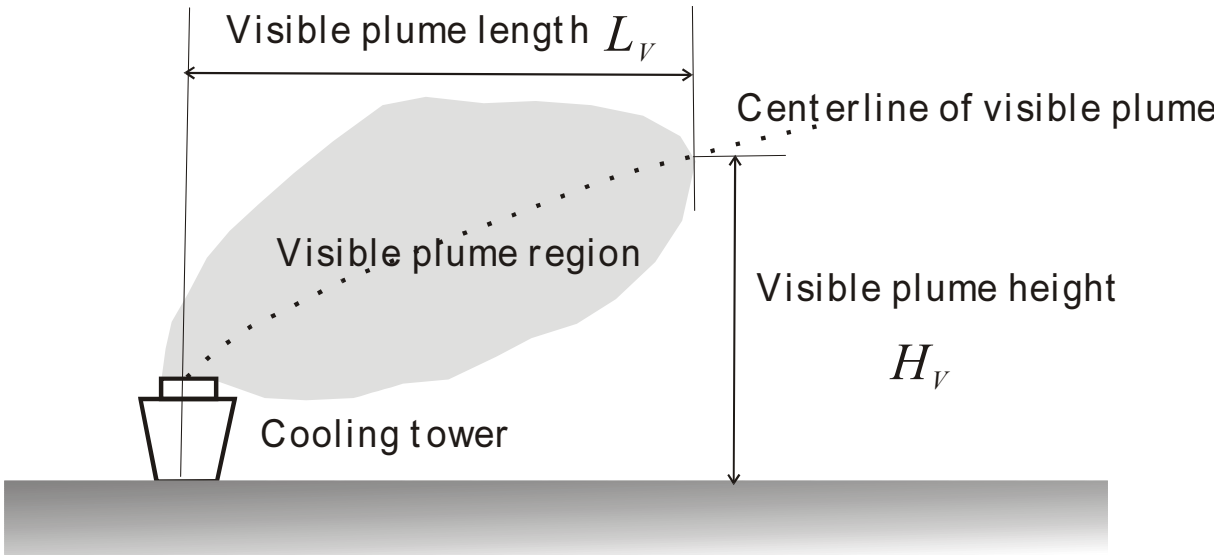

Figure 4 Definition of the visible plume region.

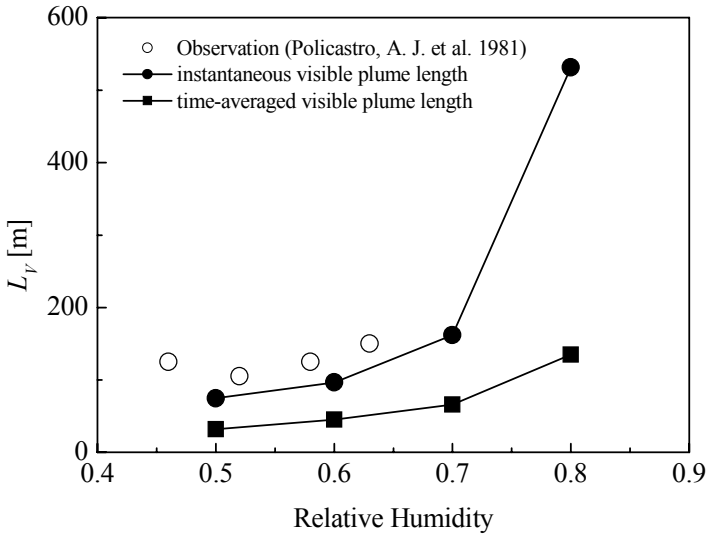

(a) Visible plume length

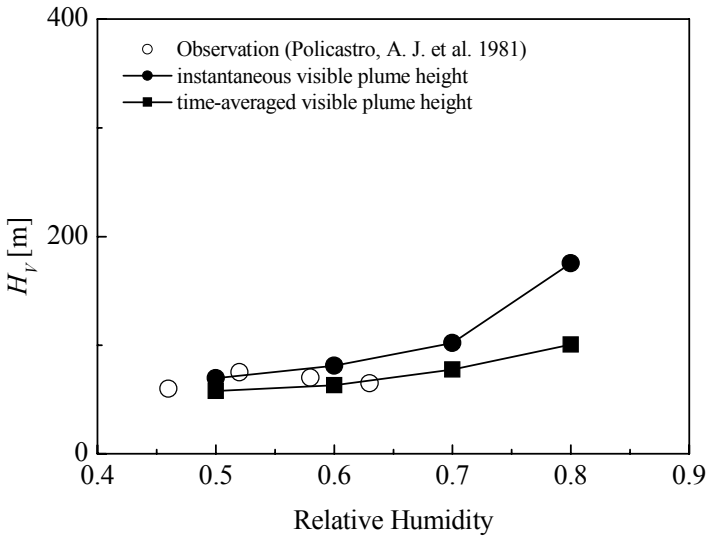

(b) Visible plume height

Figure 5 Visible plume length and height.